Impact of dietary ω3 polyunsaturated fatty acid supplementation on brown and brite adipocyte function

Rayane A. Ghandour[1], Cecilia Colson[1], Maude Giroud[2], Stefanie Maurer[3], Samah Rekima[1], Gérard Ailhaud[1], Martin Klingenspor[3], Ez-Zoubir Amri[1*] and Didier F. Pisani[1*]

[1]Université Côte d'Azur, CNRS, Inserm, iBV, France.

[2]Institute for Diabetes and Cancer (IDC), Helmholtz Zentrum, München, Germany

[3]Center for Nutritional Medicine, Technical University Munich, Freising, Germany.

[*]Corresponding authors: Dr. Didier Pisani: pisani@unice.fr and Dr. Ez-Zoubir Amri: amri@unice.fr; iBV, Institut de Biologie Valrose, Univ. Nice Sophia Antipolis, UFR Médecine, 28 avenue de Valombrose, 06107 Nice Cedex 2, France. Tel: +33 493 37 77 07; Fax: +33 493 81 70 58;

Running title. ω6/ω3 PUFA ratio effects on thermogenic adipocytes

Abbreviations: ARA: arachidonic acid; BAT: brown adipose tissue; UCP: uncoupling protein 1; WAT: white adipose tissue.

Abstract.

The recent characterization of functional brown adipose tissue (BAT) in adult humans has opened new perspectives for regulation of energy expenditure with respect to obesity and diabetes. Furthermore, dietary recommendations have taken into account the insufficient dietary intake of ω3 polyunsaturated fatty acids (PUFA) and the concomitant excessive intake of ω6 PUFA associated with the occurrence of overweight/obesity. We aimed to study whether ω3 PUFAs could play a role in the recruitment and function of energy-dissipating brown/brite adipocytes. We show that ω3 PUFA supplementation has beneficial effect on the thermogenic function of adipocytes. *In vivo*, a low dietary ω6/ω3 ratio improved the thermogenic response of brown and white adipose tissues to β3-adrenergic stimulation. This effect was recapitulated *in vitro* by PUFAs treatment of hMADS adipocytes. We pinpoint the ω6-derived eicosanoid PGF2α as the molecular origin since the effects were mimicked with a specific PGF2α receptor agonist. PGF2α level in hMADS adipocytes was reduced in response to ω3 PUFA supplementation. The recruitment of thermogenic adipocytes is influenced by the local quantity of individual oxylipins, which is controlled by the ω6/ω3 ratio of available lipids. In human nutrition, energy homeostasis may thus benefit from the implementation of a more balanced dietary ω6/ω3 ratio.

Keywords. PUFA; oxylipins; prostaglandins; adipose tissue; UCP1.

Introduction

Dietary fats are the source of essential polyunsaturated fatty acids (PUFAs), *i.e.* ω6 linoleic acid (LA), a precursor of ω6 arachidonic acid (ARA), and ω3 α-linolenic acid, a precursor of ω3 eicosapentaenoic (EPA) and docosahexaenoic (DHA) acids. These long-chain PUFAs trigger a variety of biological responses, particularly in adipose tissue, and are required for healthy development (1, 2). New dietary recommendations take into account the insufficient intake of ω3 PUFAs and the excess of ω6 PUFAs, which correlate with overweight/obesity (3-5). Indeed, high ω6/ω3 ratios are positively associated with adiposity of infants at 6 months, 3 and 4 years of age (6-8), and ARA intake correlates positively with the body mass index (BMI) and the associated metabolic syndrome (9-13). In fact, diets exhibiting a high ω6/ω3 ratio result in a higher ARA bioavailability for the synthesis of ω6 derived oxylipins due to an insufficient compensatory effect of EPA and DHA (14). These ω6 oxygenated derivatives are known to favor inflammatory responses (15), as well as to promote energy storage (16) and to inhibit energy expenditure (17). These effects are mainly triggered by oxylipins arising from the cyclooxygenase (COX) pathway.

In contrast to the white adipose tissue (WAT) involved in energy storage and release, brown adipose tissue (BAT) is endowed with a thermogenic activity and regulates body temperature by dissipating energy through non-shivering thermogenesis (18). This mechanism is mediated by the uncoupling protein 1 (UCP1), which uncouples mitochondrial oxygen consumption from energy production. Interestingly, a further population of UCP1-positive adipocytes is present in WAT and is termed brite for "brown in white" or beige adipocytes (19-21). *In vivo,* brite adipocytes stem from progenitors or emerge by direct conversion of mature white adipocytes (22-24). Several studies have demonstrated the involvement of oxylipins in fat mass development through the modulation of white and brown/brite adipocyte differentiation and activity (25). Mice exposed to diets with high levels of ω6 PUFA during the perinatal period display progressive accumulation of body fat across generations (26). This observation is in agreement with the consumption of Westernized diets rich in ω6 PUFAs as overweight and obesity develop earlier in life and have increased within a given population during the last decades (26). Moreover, oxylipins derived from ω6 PUFA inhibit brite and brown adipocyte activity both *in vitro* and *in vivo* (17). ARA lowers the expression and function of UCP1, thus affecting the dissipation

of energy in these thermogenic adipocytes. These effects are mediated *via* COX activities that lead to increased synthesis and release of PGE2 and PGF2α, which act as inhibitors of Ucp1-mediated thermogenesis via a calcium-dependent pathway.

It has been shown that healthy adult humans exhibit BAT in the cervical and thoracic part of the body, which consists in islets of energy-dissipating thermogenic adipocytes (27-31). These adipocytes display a gene expression signature comparable to either rodent brown or brite adipocytes depending on the localization and the depth of the analyzed tissue (21, 32-34). As brown and brite adipocytes represent important candidates for controlling body weight, investigations in humans on the regulation of brown/brite adipocyte recruitment and activation are in demand, particularly from a nutritional point of view since quantitative and qualitative issues of dietary lipids are relevant to increased body weight (3). As in mammals oxylipins govern a large part of the biology of adipose tissue, any dysregulation in their levels may disrupt tissue homeostasis. Thus, it is tempting to assume that prevention of excessive consumption of ω6 fatty acids or re-establishment of a balanced ω6/ω3 PUFA ratio from 30 may contribute to reduce excessive adipose tissue development by controlling white adipocyte formation and enhancing brite adipocyte recruitment.

Herein, we aimed to study whether the inhibitory effect of ω6-PUFA linoleic acid (via local action of ARA) on brite adipocyte recruitment could be reversed by supplementation with the ω3-PUFA α-linolenic acid associated to its metabolites EPA and DHA. We show, *in vivo* in mice and *in vitro* in human cells, that adjustment of a ω6/ω3 PUFA ratio from 30 to 3.7 by supplementation of ω6 PUFA-enriched diet with ω3 PUFAs rescues the inhibitory effect of ω6-derived oxylipins on the activity of brown and brite adipocytes. These effects are mediated through oxylipins via decreased level of PGF2α.

Materials and Methods

Animals and diets. The experiments were conducted in accordance with the French and European regulations (directive 2010/63/EU) for the care and use of research animals and were approved by national experimentation committees (MESR 01947.03). Ten week-old C57BL/6J male mice from Janvier Laboratory (France) were maintained at thermoneutrality (28 ± 2°C) and 12:12-hour light-dark cycles, with *ad libitum* access to food and water and killed at 10-11 AM. Mice were fed for 12 weeks with isocaloric ω6- or ω3-supplemented diets (12% energy content as lipids). These experimental diets were prepared from standard chow diets (ref. 2016, Harlan Lab., WI, USA). The ω6-supplemented diet was enriched with 0.5% linoleate-ethyl-ester (LA) and 0.7% oleate-ethyl-ester (OA) (ratio ω6/ω3 = 30); the ω3-supplemented diet comprised 0.5% LA, 0.54% α-linolenate-ethyl-ester (LNA), 0.08% eicosapentaenoate-ethyl-ester and 0.08% docosahexaenoate-ethyl-ester (ratio ω6/ω3 = 3.7) (see supplemental Table S1 for details) in order to follow human nutritional recommendations. Safflower oil (0.5%) was added to favor dispersion of ethyl esters in the diet. Fatty acid ethyl esters were from NuChekPrep (MIN, USA) and diets were produced by Harlan (WI, USA). Chronic β_3-adrenergic receptor stimulation was carried out during the last week of the diet treatment by daily intra-peritoneal injections of CL316,243 (1 mg/kg in saline solution). Control mice were injected with vehicle only. Blood, interscapular BAT (iBAT), epididymal (eWAT) and inguinal subcutaneous WAT (scWAT) were sampled and used for different analyses.

hMADS cell culture. The establishment and characterization of hMADS cells has been described (35-37). In the experiments reported herein, hMADS-3 cells were used between passages 14 and 20. All experiments were performed at least 3 times using different cultures. Cells were cultured and differentiated as previously described (17, 35). Briefly, cells were induced to differentiate at day 2 post-confluence (designated as day 0) in DMEM/Ham's F12 media supplemented with 10 µg/ml transferrin, 10 nM insulin, 0.2 nM triiodothyronine, 1 µM dexamethasone and 500 µM isobutyl-methylxanthine (IBMX). Two days later, the medium was changed (dexamethasone and IBMX omitted) and 100 nM rosiglitazone was added. At day 9 rosiglitazone was withdrawn to enable white adipocyte differentiation but again included between days 14 and 17 to promote white to brite adipocyte conversion as previously

described (17, 35). Fatty acids were bound to bovine serum albumin (BSA) (0.04% for 15 min at 37°C) prior to addition to culture media.

Oxylipin quantification. *In vitro* analysis of secreted PGF2α was performed on differentiated cells at day 17 after incubation for 1 or 24 h in fresh culture media. PGF2α was quantified by Elisa Immuno Assay (EIA) following the manufacturer's instructions (Cayman, BertinPharma, Montigny le Bretonneux, France).

Quantification of oxylipins was performed at METATOUL platform (MetaboHUB, INSERM UMR 1048, I2MC, Toulouse, France) by mass spectrometry analysis. All tissues were snap-frozen with liquid nitrogen immediately after collection and stored at -80°C until extraction. Extraction and analysis were performed as previously described (17, 38).

Measurement of oxygen consumption. Oxygen consumption rate (OCR) of hMADS adipocytes was determined at day 17 using an XF24 Extracellular Flux Analyzer (Seahorse Bioscience, Agilent). ATP synthase uncoupled OCR was determined by addition of 1.2 µM oligomycin A (ATP synthase inhibitor) and maximal OCR by addition of 1 µM FCCP (Carbonyl cyanide 4-(trifluoromethoxy) phenylhydrazone as a mitochondrial oxidative phosphorylation uncoupling agent). Rotenone and Antimycin A (2 µM each) were used to inhibit Complex I- and Complex III-dependent respiration, respectively. Parameters were measured for each individual well using the different value of OCR as previously described (39).

Histology. Histological analysis was performed as previously described (17). Sections (4 µm) were dewaxed and treated in boiling citrate buffer (10 mM, pH 6.0) for 6 min. Cooled sections were rinsed and then permeabilized in PBS 0.2 % triton X-100 at room temperature for 20 min. Sections were saturated in the same buffer containing 3% BSA for 30 min, incubated with perilipin antibody (#RDI-PROGP29, Research Diagnostic Inc., Flanders, USA) for 1h, and TRITC-coupled anti-guinea pig antibody for 45 min. Nuclear staining was performed with DAPI.

UCP1 immunohistochemistry was performed following manufacturer's instructions (LSAB+ system-HRP, Dako, Les Ulis, France) and using goat anti-UCP1 (clone C-17, Santa Cruz, Tebu-bio, Le Perray-

en-Yvelines, France).Visualization was performed with an Axiovert microscope and pictures were captured with AxioVision software (Carl Zeiss, Jena, Germany). Lipid droplet diameters (visualized by perilipin staining) were measured using Fiji software (40). Displayed pictures are representative of the 4 mice per group analyzed.

Isolation and analysis of RNA. These procedures follow MIQE recommendations (41). Total RNA was extracted using TRI-Reagent kit (Euromedex, Souffelweyersheim, France) according to the manufacturer's instructions. For RNA isolation from organs, tissues were homogenized in TRI-Reagent using a dispersing instrument (ULTRA TURRAX T25, Ika, Germany). Reverse transcription-polymerase chain reaction (RT-PCR) was performed using M-MLV-RT (Promega). SYBR qPCR premix Ex TaqII from Takara (Ozyme, France) was used for quantitative PCR (qPCR), and assays were run on a StepOne Plus ABI real-time PCR machine (PerkinElmer Life and Analytical Sciences, Boston). The expression of selected genes was normalized to that of the TATA-box binding protein (TBP) and 36B4 housekeeping genes for human genes, and 36B4 and Glyceraldehyde-3-phosphate dehydrogenase (GAPDH) for mouse genes, and then quantified using the comparative-ΔCt method. Primer sequences are available upon request.

Statistical analysis. Data are expressed as mean values ± SEM and were analyzed using InStat software (GraphPad Software). Data were analyzed by one-way ANOVA followed by a Student-Newman-Keuls post-test, or Student's *t*-test to assess statistical differences between experimental groups. Differences were considered statistically significant with $p<0.01$.

Results

ω3 PUFA supplementation makes mice sensitive to β3-adrenergic receptor agonist treatment.

Ten-week old mice were fed for 12 weeks with an isocaloric standard diet enriched in ω6 PUFAs (ω6 diet, ω6/ω3 = 30), or supplemented with ω3 PUFAs (ω3 diet, ω6/ω3 = 3.7) (Supplemental Table S1). There was no difference in body weight (Figure 1A) and food intake during 12 weeks (ω6 diet, 4.49 g/day *vs* ω3 diet, 4.46 g/day per mouse). During the last week, mice received daily injections of the agonist CL316,243 (1 mg/kg) to activate the β3-adrenergic receptor pathway. As expected, such treatment decreased body weight (Figure 1A) as well as interscapular BAT and epididymal WAT (eWAT) mass (Figure 1B). Interestingly, ω3 diet-fed mice showed a larger decrease in body mass and adipose tissue mass upon CL316,243-treatment compared to ω6 diet-fed mice (Figure 1A and 1B). This observation is in line with higher plasma glycerol levels (Figure 1C). Altogether, these results indicate a higher sensitivity of ω3 diet-fed mice to CL316,243 treatment.

ω3 diet-fed mice showed an improved response to thermogenic stimulation in BAT and scWAT.

After CL316,243 treatment, mice fed the ω3-diet displayed an increase in BAT mass loss and in the plasma glycerol level, suggesting a higher lipolysis capacity. As expected, histological analysis of BAT showed clear activation of brown adipocytes after CL316,243 treatment as indicated by adipocyte morphological changes in the two groups of mice (Figure 2A). This observation was confirmed by immunostaining for perilipin 1 (PLN1), a known lipid droplet surface protein, which allowed the measure of droplet diameters. The data showed smaller lipid droplets in BAT of mice treated with CL316,243 (Figure 2C). Interestingly, the droplet size was smaller in ω3 compared to ω6 diet-fed mice of both treatment groups (Figure 2C). These morphological modifications were in line with elevated expression of brown adipocyte marker genes in ω3 *vs.* ω6 diet-fed mice (Figure 2B and D).

The β3-adrenergic agonist CL316,243 is a potent inducer of brite adipocytes and therefore we hypothesized a contribution of these thermogenic cells to CL316,243-induced plasma glycerol levels and body weight loss. No morphological or gene expression differences were found in scWAT between the 2 groups of mice in response to vehicle treatment (Figure 3A and B). However, after CL316,243 treatment, visual examination of sections suggested increased Ucp1 positive adipocytes in scWAT of

ω3 diet-fed mice compared to ω6 diet-fed mice (Figure 3A). This observation was supported by the analysis of Ucp1 mRNA expression, which tended to be increased in the ω3 diet-fed group after CL316,243 treatment. Gene expression of other markers in response to CL316,243 was not affected by the diet (Figure 3B). As shown in Supplemental Figure S1, eWAT did not display multiloculated adipocytes which are characteristic of UCP1+ adipocytes. However, a decrease of adipocyte mean diameter after CL316,243 treatment was found in both groups in agreement with, eWAT weight decrease (Figure 1B).

Altogether, these data indicate that the dietary ω6/ω3 ratio affects the induction/activation of thermogenic adipocytes in BAT and scWAT upon stimulation with a β-adrenergic agonist. As the dietary fatty acid composition can considerably influence the quality and quantity of fatty acid metabolites (2, 5) this differential response to thermogenic stimulation may be the consequence of a modulated eicosanoid level in adipose tissues.

Dietary ω3 PUFA supplementation controls the level of ω6-derived oxylipins

To investigate diet-induced differences in the quantity of ω3- and ω6-derived oxylipins, we quantified the levels of more than 30 selected metabolites in scWAT and iBAT from ω3 and ω6 diet-fed mice. Depending on their origin, oxygenated metabolites derived from ω6 (ARA) or ω3 (EPA and/or DHA) PUFAs, due to COX, LOX and CYP450 activities (Supplemental Figure S2A and B, left panels, oxylipins) or to COX activity only (right panels, eicosanoids: a group of oxylipins) were analyzed (analyzed oxylipins detailed in Supplemental Table S2).

As expected, ω3 PUFAs supplementation allowed higher quantity of their metabolites in BAT and scWAT (Supplemental Figure S2A and B, black columns). In BAT, where the molecular effect of a ω3-diet was the most important, we did not find any significant impact of the diet on ω6-derived oxylipin levels (Supplemental Figure S2A, grey columns). In scWAT, similar data were obtained in untreated mice, however when the mice were treated with the β3-adrenergic receptor agonist, the decrease in the levels of ω6-derived oxylipins was higher in ω3 diet-fed mice than in ω6-diet fed mice (Supplemental Figure S2).

Analysis of COX derived eicosanoids showed an increase in EPA derived eicosanoids in the ω3 diet-fed group and no significant decrease of ω6-derived eicosanoids, except after CL316,243 treatment (Supplemental Figure S2A and B, right panels). Of note, the treatment with CL316,243, a situation where the UCP1 activity is increased *via* the release of fatty acids, led to a decrease in the levels of the various oxygenated metabolites, possibly reflecting the preferential use of PUFAs as fuel for thermogenesis, thus limiting their availability for oxylipin production (Figure 4 and Supplemental Figure S2).

Previous work from our laboratory has demonstrated that COX-derived oxylipins are crucial for the formation and activation of thermogenic adipocytes (17, 42). Accordingly, further analyses focused on the levels of individual COX-derived oxylipins (*i.e.* 6kPGF1α (representative of PGI2), PGF2α, PGE2, TXB2, PGD2 and 15dPGJ2) in BAT and scWAT. The levels of most individual metabolites were similar in iBAT and scWAT of vehicle-treated ω6 diet- and ω3 diet-fed mice, except for a decrease in TXB2 levels in BAT and in PGE2 levels in scWAT (Figure 4A and B). Treatment with CL316,243 resulted in decreased quantity of these oxylipins in both diet groups in BAT and scWAT, although down regulation of TXB2 and PGE2 was more pronounced in scWAT than in iBAT. Interestingly, PGF2α was exempt from this mode of regulation: CL316,243-treatment resulted in a significant decrease in PGF2α level in ω3 diet-fed but not in ω6 diet-fed mice. Thus, the level of this eicosanoid in response to CL316,243-treatment is inversely correlated with Ucp1 expression in BAT and scWAT.

Our previous results demonstrated (17) that PGF2α is a negative regulator of thermogenic adipocyte recruitment. Indeed, the ω6-enriched diet PGF2α level was not affected by CL316,243 treatment (Figure 4A and B) and correlated with inhibition of brown and brite adipocyte recruitment and activation (Figures 2 and 3). In contrast, for a ω3-enriched diet, after CL316,243 treatment, no alteration in the brown and brite adipocyte recruitment and activation was found though a striking decrease in the PGF2α level was observed (Figure 4A and B).

Taken together these results demonstrated that diet supplementation with ω3 PUFAs reversed the inhibitory effect of a ω6-enriched diet. This effect could be due to competition between ω6 and ω3 PUFAs at the COX activity level leading in turn to a decrease in PGF2α synthesis. To further investigate

the effect of PUFAs and eicosanoids on adipocyte function, we used brite adipocytes derived from hMADS cells as a model system.

EPA reversed the ARA-inhibitory effect *in vitro*.

hMADS cells are a human stem cell model that is able to differentiate into white adipocytes and to convert into functional brite adipocytes upon rosiglitazone treatment (Figure 5A, (17, 35)). As described previously (17), this process can be modified by ω6-PUFA ARA: treatment of hMADS adipocytes during the conversion to brite adipocytes with ARA inhibited the expression of UCP1 and other brite adipocyte markers (CIDEA, CPT1M, PLN5) (Figure 5A). Such treatment did not affect adipogenesis *per se*, as the expression of PLN1 and ADIPQ was not affected (Figure 5A). Treatment of hMADS adipocytes with the ω3-PUFA EPA (molar ARA/EPA ratio of 3) reversed the inhibitory effect of ARA on brite adipocyte marker expression (Figure 5A). This effect was further investigated at the functional level. Oxygen consumption analysis of hMADS brite adipocytes revealed that ARA inhibited all mitochondrial respiration parameters (Figure 5B), *i.e.* basal, uncoupled and maximal respiration as well as the spare respiratory capacity (SRC). EPA partially reversed this inhibitory effect of ARA on mitochondrial oxygen consumption, thus affecting the overall thermogenic capacity of these cells (Figure 5B). No change in adipogenic marker expression was observed when DHA was added as an alternative ω3 PUFA (Supplemental Figure S3) indicating EPA to specifically represent the effective compound within this class of molecules.

Taken together these results indicated the thermogenic function of adipocytes to be positively and negatively affected by EPA (ω3) and ARA (ω6), respectively.

EPA reduced PGF2α synthesis and secretion.

To identify the pathway involved in the EPA effect, we used fluprostenol, an agonist of the FP receptor (PGF2α receptor), instead of the precursor ARA during the conversion of white hMADS adipocytes into brite adipocytes. In agreement with our previous work (17), fluprostenol mimicked the effect of ARA by inhibiting the expression of UCP1 mRNA (Figure 6A). Co-treatment with EPA did not reverse this effect (Figure 6A), indicating that the UCP1 expression of brite hMADS adipocytes was directly

affected by an interaction between the FP receptor and its ω6-derived, endogenous ligand PGF2α. Thus, we hypothesized that EPA reversed the ARA-induced effects in brite hMADS adipocytes by modulating the availability of PGF2α as ligand for its receptor. Accordingly, we measured PGF2α secretion after ARA treatment of brite hMADS adipocytes in the absence or presence of EPA. PGF2α secretion, was not altered by EPA during the first hour of treatment. However, a striking decrease in PGF2α levels was observed after 24 h (Figure 6B). This decrease in quantity was likely not due to a lower expression of the major enzymes involved in PGF2α synthesis. Indeed, the expression of COX-1, COX-2 (allowing the metabolization of ARA to PGG2), AKR1B1 and AKR1C3 (allowing the metabolization of PGG2 to PGF2α) mRNAs was not altered by EPA treatment (Figure 6C). As both ARA and EPA can be recognized and metabolized by COX-1 and COX-2, EPA most likely blocks PGF2α synthesis by competing with ARA.

Discussion

The obesogenic effect of ω6 PUFAs, particularly ARA, is thought to originate from their metabolization to oxylipins thus promoting fat storage and a reduction in energy expenditure (16, 17, 43, 44). However, this system and its regulation appear to underlie an unanticipated complexity. In fact, previous studies demonstrated the ω6 eicosanoid prostacyclin (PGI2, which is derived from ARA via COX-dependent metabolization) as a positive modulator of UCP1 expression and brite adipogenesis in human and murine cellular model systems (42, 45-47). In line with these findings, transgenic mice with constitutive overexpression of COX-2 (the inducible isoform of COX) show enhanced browning of WAT and resistance to diet-induced obesity (46). The complexity of this system becomes apparent in IP receptor knockout mice, which are protected from ω6 PUFA-induced body and fat mass gain (16). In a similar way, when mice were fed a high fat diet, the inhibition of COX activities with indomethacin prevented body weight gain, due to decreased fat storage and enhanced recruitment of brite adipocytes in the scWAT (15, 43). These examples emphasize the need to increase our current understanding of the pro- and anti-adipogenic properties of PUFAs on the level of oxylipin metabolism to modulate energy balance regulation.

In our previous work, we elucidated in more detail the relationship between ARA-derived eicosanoid level, browning of WAT and energy expenditure. Mice were fed an ARA-supplemented standard diet and showed impaired brown adipocyte activation and brite adipocyte recruitment in response to CL316,243 treatment, an effect that was attributed to the abundance of PGF2α (17). Using hMADS adipocytes as an *in vitro* cell model, we demonstrated that this eicosanoid translates its inhibitory effect on the thermogenic capacity of adipocytes via an interaction with its natural cell surface receptor, the FP receptor, upon its synthesis from ARA via COX activity (17). Herein we show that this ARA-dependent production of PGF2α is attenuated in the presence of ω3-PUFAs both *in vitro* in brite hMADS adipocytes and *in vivo* in thermogenically activated brown and brite adipocytes. We conclude that Ucp1 expression in these models is less affected by the elevated quantity of ω3-derived metabolites but rather depends on the reduced level of individual ω6-derived metabolites (such as PGF2α) with EPA-treatment.

Both ω6 and ω3 PUFAs are transported in the bloodstream between tissues and are incorporated in plasma membrane under the form of phospholipids or as triglycerides within adipocytes (48-50). PUFAs are released into the cell by lipases and metabolized into oxylipins using similar pathways. ω6 and ω3 PUFAs are known to compete at different steps that modulate the availability of their respective metabolites. LA and LNA use the same Δ-desaturases and elongases to generate PUFA metabolites such as ARA, DGLA (Dihomo-γ-linolenic acid), EPA and DHA (51). They can also be used as substrates *via* β-oxidation, ω3 PUFAs being more rapidly oxidized compared to ω6 PUFAs and mono-unsaturated fatty acids (52).

Although our data support a model in which dietary PUFAs act on the level of oxylipins, this mechanism is not exclusive in the context of thermogenic adipocyte recruitment since ω3-PUFAs per se are associated with browning properties (53, 54). For example, when mice or rats are fed a LA-enriched diet, the increase in fat mass can be prevented by LNA supplementation under isolipidic and isocaloric conditions (16, 55, 56). Using this strategy, we demonstrated herein that ω3 PUFA diet supplementation ameliorates brown adipocyte function in response to β-adrenergic stimulation, by promoting a more oxidative phenotype and to a lesser extent brite adipocyte recruitment. Analysis of PUFA metabolites associated to this improvement showed a decrease in the n-2 series prostaglandins levels, especially PGF2α. Altogether, *in vivo* and *in vitro* data show that the competition between ω6 and ω3 PUFAs takes place at the level of COX activities, favoring the production of EPA-derived metabolites instead of ARA-derived metabolites. DHA treatment was inefficient. The lack of effect could be due to the fact that DHA does not compete with ARA for metabolite production but was described to inhibit activity and expression of COX-2 (57).

Interestingly, this mechanism does not appear to contribute to the regulation of body weight when mice are fed under thermoneutral conditions but rapidly initiates the mobilization of fat as an energy substrate in response to thermogenic stimulation. This observation may be of particular relevance to the treatment of overweight and obesity in human subjects as humans constantly live in a thermoneutral environment. Thus, adjusting the ω6/ω3-ratio of human nutrition according to dietary recommendations may benefit the recruitment of brown and brite adipocytes associated with other therapeutic strategies in order to promote a negative energy balance.

Supporting the physiological relevance of ω3 PUFA-induced effects, fish oil supplementation has been reported to induce UCP1 expression via the sympathetic nervous system, although this mechanism is restricted to BAT (58, 59).

In conclusion, herein we demonstrate that ω3 PUFA supplementation compensates for the inhibitory effect of ω6 PUFAs on the thermogenic function of adipocytes. We identified the eicosanoid PGF2α as a causal effector, the level of which is influenced by the availability of ω6 and ω3 PUFAs competing at the level of their metabolization. Our data indicate that the dietary ω6/ω3 ratio is a major regulator of adaptive thermogenesis consequently affecting energy homeostasis. These findings are of particular importance in a human nutritional context as the dietary ω6/ω3 ratio is associated with the development of obesity, cardiovascular and inflammatory diseases.

Acknowledgments/grant support. The authors greatly acknowledge the IRCAN Animal core facilitiy and the Cytomed platform as well as the IBV histology platform. We thank Pauline Le Faouder and Justine Bertrand-Michel from the METATOUL platform (MetaboHUB, INSERM UMR 1048, I2MC, Toulouse, France) for oxylipins analysis. We thank Amanda Balzo and Clémence Auverdin for their technical suport. This work was supported by CNRS, French Agence Nationale de la Recherche and Deutsche Forschungsgemeinschaft (ANR/DFG-15-CE14-0033 "Nutribrite") and Nutricia Research Foundation ("2015-26"). The manuscript has been corrected by Dr. Brahimi-Horn (EditDocSci, http://cbrahimihorn.free.fr), a native English speaking scientific editor.

References

1. Simopoulos, A. P. 2002. The importance of the ratio of omega-6/omega-3 essential fatty acids. *Biomed. Pharmacother.* **56**: 365-379.
2. Simopoulos, A. P. 2016. An Increase in the Omega-6/Omega-3 Fatty Acid Ratio Increases the Risk for Obesity. *Nutrients* **8**: 128.
3. Ailhaud, G., F. Massiera, P. Weill, P. Legrand, J. M. Alessandri, and P. Guesnet. 2006. Temporal changes in dietary fats: role of n-6 polyunsaturated fatty acids in excessive adipose tissue development and relationship to obesity. *Prog. Lipid Res.* **45**: 203-236.
4. Muhlhausler, B. S., and G. P. Ailhaud. 2013. Omega-6 polyunsaturated fatty acids and the early origins of obesity. *Curr. Opin. Endocrinol. Diabetes Obes.* **20**: 56-61.
5. Simopoulos, A. P., and J. J. DiNicolantonio. 2016. The importance of a balanced omega-6 to omega-3 ratio in the prevention and management of obesity. *Open Heart* **3**: e000385.
6. Donahue, S. M., S. L. Rifas-Shiman, D. R. Gold, Z. E. Jouni, M. W. Gillman, and E. Oken. 2011. Prenatal fatty acid status and child adiposity at age 3 y: results from a US pregnancy cohort. *Am. J. Clin. Nutr.* **93**: 780-788.
7. Moon, R. J., N. C. Harvey, S. M. Robinson, G. Ntani, J. H. Davies, H. M. Inskip, K. M. Godfrey, E. M. Dennison, P. C. Calder, C. Cooper, and S. W. S. S. Group. 2013. Maternal plasma polyunsaturated fatty acid status in late pregnancy is associated with offspring body composition in childhood. *J. Clin. Endocrinol. Metab.* **98**: 299-307.
8. Rudolph, M. C., B. E. Young, D. J. Lemas, C. E. Palmer, T. L. Hernandez, L. A. Barbour, J. E. Friedman, N. F. Krebs, and P. S. MacLean. 2017. Early infant adipose deposition is positively associated with the n-6 to n-3 fatty acid ratio in human milk independent of maternal BMI. *Int. J. Obes. (Lond.)* **41**: 510-517.

9. Inoue, K., K. Kishida, A. Hirata, T. Funahashi, and I. Shimomura. 2013. Low serum eicosapentaenoic acid / arachidonic acid ratio in male subjects with visceral obesity. *Nutr Metab (Lond)* **10**: 25.

10. Savva, S. C., C. Chadjigeorgiou, C. Hatzis, M. Kyriakakis, G. Tsimbinos, M. Tornaritis, and A. Kafatos. 2004. Association of adipose tissue arachidonic acid content with BMI and overweight status in children from Cyprus and Crete. *Br. J. Nutr.* **91**: 643-649.

11. Williams, E. S., A. Baylin, and H. Campos. 2007. Adipose tissue arachidonic acid and the metabolic syndrome in Costa Rican adults. *Clin. Nutr.* **26**: 474-482.

12. Claria, J., B. T. Nguyen, A. L. Madenci, C. K. Ozaki, and C. N. Serhan. 2013. Diversity of lipid mediators in human adipose tissue depots. *Am. J. Physiol. Cell Physiol.* **304**: C1141-1149.

13. Garaulet, M., F. Perez-Llamas, M. Perez-Ayala, P. Martinez, F. S. de Medina, F. J. Tebar, and S. Zamora. 2001. Site-specific differences in the fatty acid composition of abdominal adipose tissue in an obese population from a Mediterranean area: relation with dietary fatty acids, plasma lipid profile, serum insulin, and central obesity. *Am. J. Clin. Nutr.* **74**: 585-591.

14. Fischer, R., A. Konkel, H. Mehling, K. Blossey, A. Gapelyuk, N. Wessel, C. von Schacky, R. Dechend, D. N. Muller, M. Rothe, F. C. Luft, K. Weylandt, and W. H. Schunck. 2014. Dietary omega-3 fatty acids modulate the eicosanoid profile in man primarily via the CYP-epoxygenase pathway. *J. Lipid Res.* **55**: 1150-1164.

15. Ghoshal, S., D. B. Trivedi, G. A. Graf, and C. D. Loftin. 2011. Cyclooxygenase-2 deficiency attenuates adipose tissue differentiation and inflammation in mice. *J. Biol. Chem.* **286**: 889-898.

16. Massiera, F., P. Saint-Marc, J. Seydoux, T. Murata, T. Kobayashi, S. Narumiya, P. Guesnet, E. Z. Amri, R. Negrel, and G. Ailhaud. 2003. Arachidonic acid and prostacyclin

signaling promote adipose tissue development: a human health concern? *J. Lipid Res.* **44**: 271-279.

17. Pisani, D. F., R. A. Ghandour, G. E. Beranger, P. Le Faouder, J. C. Chambard, M. Giroud, A. Vegiopoulos, M. Djedaini, J. Bertrand-Michel, M. Tauc, S. Herzig, D. Langin, G. Ailhaud, C. Duranton, and E. Z. Amri. 2014. The omega6-fatty acid, arachidonic acid, regulates the conversion of white to brite adipocyte through a prostaglandin/calcium mediated pathway. *Molecular metabolism* **3**: 834-847.
18. Cannon, B., and J. Nedergaard. 2004. Brown adipose tissue: function and physiological significance. *Physiol. Rev.* **84**: 277-359.
19. Petrovic, N., T. B. Walden, I. G. Shabalina, J. A. Timmons, B. Cannon, and J. Nedergaard. 2010. Chronic peroxisome proliferator-activated receptor gamma (PPARgamma) activation of epididymally derived white adipocyte cultures reveals a population of thermogenically competent, UCP1-containing adipocytes molecularly distinct from classic brown adipocytes. *J. Biol. Chem.* **285**: 7153-7164.
20. Ishibashi, J., and P. Seale. 2010. Medicine. Beige can be slimming. *Science* **328**: 1113-1114.
21. Wu, J., P. Bostrom, L. M. Sparks, L. Ye, J. H. Choi, A. H. Giang, M. Khandekar, K. A. Virtanen, P. Nuutila, G. Schaart, K. Huang, H. Tu, W. D. van Marken Lichtenbelt, J. Hoeks, S. Enerback, P. Schrauwen, and B. M. Spiegelman. 2012. Beige adipocytes are a distinct type of thermogenic fat cell in mouse and human. *Cell* **150**: 366-376.
22. Barbatelli, G., I. Murano, L. Madsen, Q. Hao, M. Jimenez, K. Kristiansen, J. P. Giacobino, R. De Matteis, and S. Cinti. 2010. The emergence of cold-induced brown adipocytes in mouse white fat depots is determined predominantly by white to brown adipocyte transdifferentiation. *Am. J. Physiol. Endocrinol. Metab.* **298**: E1244-1253.

23. Lee, Y. H., E. P. Mottillo, and J. G. Granneman. 2014. Adipose tissue plasticity from WAT to BAT and in between. *Biochim. Biophys. Acta* **1842**: 358-369.

24. Rosenwald, M., A. Perdikari, T. Rulicke, and C. Wolfrum. 2013. Bi-directional interconversion of brite and white adipocytes. *Nat. Cell Biol.* **15**: 659-667.

25. Barquissau, V., R. A. Ghandour, G. Ailhaud, M. Klingenspor, D. Langin, E. Z. Amri, and D. F. Pisani. 2017. Control of adipogenesis by oxylipins, GPCRs and PPARs. *Biochimie* **136**: 3-11.

26. Massiera, F., P. Barbry, P. Guesnet, A. Joly, S. Luquet, C. Moreilhon-Brest, T. Mohsen-Kanson, E. Z. Amri, and G. Ailhaud. 2010. A Western-like fat diet is sufficient to induce a gradual enhancement in fat mass over generations. *J. Lipid Res.* **51**: 2352-2361.

27. Cypess, A. M., S. Lehman, G. Williams, I. Tal, D. Rodman, A. B. Goldfine, F. C. Kuo, E. L. Palmer, Y. H. Tseng, A. Doria, G. M. Kolodny, and C. R. Kahn. 2009. Identification and importance of brown adipose tissue in adult humans. *N. Engl. J. Med.* **360**: 1509-1517.

28. Nedergaard, J., T. Bengtsson, and B. Cannon. 2007. Unexpected evidence for active brown adipose tissue in adult humans. *Am. J. Physiol. Endocrinol. Metab.* **293**: E444-452.

29. Saito, M., Y. Okamatsu-Ogura, M. Matsushita, K. Watanabe, T. Yoneshiro, J. Nio-Kobayashi, T. Iwanaga, M. Miyagawa, T. Kameya, K. Nakada, Y. Kawai, and M. Tsujisaki. 2009. High incidence of metabolically active brown adipose tissue in healthy adult humans: effects of cold exposure and adiposity. *Diabetes* **58**: 1526-1531.

30. van Marken Lichtenbelt, W. D., J. W. Vanhommerig, N. M. Smulders, J. M. Drossaerts, G. J. Kemerink, N. D. Bouvy, P. Schrauwen, and G. J. Teule. 2009. Cold-activated brown adipose tissue in healthy men. *N. Engl. J. Med.* **360**: 1500-1508.

31. Virtanen, K. A., M. E. Lidell, J. Orava, M. Heglind, R. Westergren, T. Niemi, M. Taittonen, J. Laine, N. J. Savisto, S. Enerback, and P. Nuutila. 2009. Functional brown adipose tissue in healthy adults. *N. Engl. J. Med.* **360**: 1518-1525.

32. Cypess, A. M., A. P. White, C. Vernochet, T. J. Schulz, R. Xue, C. A. Sass, T. L. Huang, C. Roberts-Toler, L. S. Weiner, C. Sze, A. T. Chacko, L. N. Deschamps, L. M. Herder, N. Truchan, A. L. Glasgow, A. R. Holman, A. Gavrila, P. O. Hasselgren, M. A. Mori, M. Molla, and Y. H. Tseng. 2013. Anatomical localization, gene expression profiling and functional characterization of adult human neck brown fat. *Nat. Med.* **19**: 635-639.

33. Jespersen, N. Z., T. J. Larsen, L. Peijs, S. Daugaard, P. Homoe, A. Loft, J. de Jong, N. Mathur, B. Cannon, J. Nedergaard, B. K. Pedersen, K. Moller, and C. Scheele. 2013. A classical brown adipose tissue mRNA signature partly overlaps with brite in the supraclavicular region of adult humans. *Cell metabolism* **17**: 798-805.

34. Sharp, L. Z., K. Shinoda, H. Ohno, D. W. Scheel, E. Tomoda, L. Ruiz, H. Hu, L. Wang, Z. Pavlova, V. Gilsanz, and S. Kajimura. 2012. Human BAT possesses molecular signatures that resemble beige/brite cells. *PLoS One* **7**: e49452.

35. Pisani, D. F., M. Djedaini, G. E. Beranger, C. Elabd, M. Scheideler, G. Ailhaud, and E. Z. Amri. 2011. Differentiation of Human Adipose-Derived Stem Cells into "Brite" (Brown-in-White) Adipocytes. *Front. Endocrinol. (Lausanne)* **2**: 87.

36. Rodriguez, A. M., C. Elabd, F. Delteil, J. Astier, C. Vernochet, P. Saint-Marc, J. Guesnet, A. Guezennec, E. Z. Amri, C. Dani, and G. Ailhaud. 2004. Adipocyte differentiation of multipotent cells established from human adipose tissue. *Biochem. Biophys. Res. Commun.* **315**: 255-263.

37. Elabd, C., C. Chiellini, M. Carmona, J. Galitzky, O. Cochet, R. Petersen, L. Penicaud, K. Kristiansen, A. Bouloumie, L. Casteilla, C. Dani, G. Ailhaud, and E. Z. Amri. 2009. Human multipotent adipose-derived stem cells differentiate into functional brown adipocytes. *Stem Cells* **27**: 2753-2760.

38. Le Faouder, P., V. Baillif, I. Spreadbury, J. P. Motta, P. Rousset, G. Chene, C. Guigne, F. Terce, S. Vanner, N. Vergnolle, J. Bertrand-Michel, M. Dubourdeau, and N. Cenac. 2013.

LC-MS/MS method for rapid and concomitant quantification of pro-inflammatory and pro-resolving polyunsaturated fatty acid metabolites. *J. Chromatogr. B Analyt. Technol. Biomed. Life Sci.* **932**: 123-133.

39. Brand, M. D., and D. G. Nicholls. 2011. Assessing mitochondrial dysfunction in cells. *Biochem. J.* **435**: 297-312.
40. Schindelin, J., I. Arganda-Carreras, E. Frise, V. Kaynig, M. Longair, T. Pietzsch, S. Preibisch, C. Rueden, S. Saalfeld, B. Schmid, J. Y. Tinevez, D. J. White, V. Hartenstein, K. Eliceiri, P. Tomancak, and A. Cardona. 2012. Fiji: an open-source platform for biological-image analysis. *Nat Methods* **9**: 676-682.
41. Bustin, S. A., V. Benes, J. A. Garson, J. Hellemans, J. Huggett, M. Kubista, R. Mueller, T. Nolan, M. W. Pfaffl, G. L. Shipley, J. Vandesompele, and C. T. Wittwer. 2009. The MIQE guidelines: minimum information for publication of quantitative real-time PCR experiments. *Clin. Chem.* **55**: 611-622.
42. Ghandour, R. A., M. Giroud, A. Vegiopoulos, S. Herzig, G. Ailhaud, E. Z. Amri, and D. F. Pisani. 2016. IP-receptor and PPARs trigger the conversion of human white to brite adipocyte induced by carbaprostacyclin. *Biochim. Biophys. Acta* **1861**: 285-293.
43. Fjaere, E., U. L. Aune, K. Roen, A. H. Keenan, T. Ma, K. Borkowski, D. M. Kristensen, G. W. Novotny, T. Mandrup-Poulsen, B. D. Hudson, G. Milligan, Y. Xi, J. W. Newman, F. G. Haj, B. Liaset, K. Kristiansen, and L. Madsen. 2014. Indomethacin Treatment Prevents High Fat Diet-induced Obesity and Insulin Resistance but Not Glucose Intolerance in C57BL/6J Mice. *J. Biol. Chem.* **289**: 16032-16045.
44. Javadi, M., H. Everts, R. Hovenier, S. Kocsis, A. E. Lankhorst, A. G. Lemmens, J. T. Schonewille, A. H. Terpstra, and A. C. Beynen. 2004. The effect of six different C18 fatty acids on body fat and energy metabolism in mice. *Br. J. Nutr.* **92**: 391-399.

45. Mossenbock, K., A. Vegiopoulos, A. J. Rose, T. P. Sijmonsma, S. Herzig, and T. Schafmeier. 2014. Browning of white adipose tissue uncouples glucose uptake from insulin signaling. *PLoS One* **9**: e110428.

46. Vegiopoulos, A., K. Muller-Decker, D. Strzoda, I. Schmitt, E. Chichelnitskiy, A. Ostertag, M. Berriel Diaz, J. Rozman, M. Hrabe de Angelis, R. M. Nusing, C. W. Meyer, W. Wahli, M. Klingenspor, and S. Herzig. 2010. Cyclooxygenase-2 controls energy homeostasis in mice by de novo recruitment of brown adipocytes. *Science* **328**: 1158-1161.

47. Babaei, R., I. Bayindir-Buchhalter, I. Meln, and A. Vegiopoulos. 2017. Immuno-Magnetic Isolation and Thermogenic Differentiation of White Adipose Tissue Progenitor Cells. *Methods Mol. Biol.* **1566**: 37-48.

48. Fickova, M., P. Hubert, G. Cremel, and C. Leray. 1998. Dietary (n-3) and (n-6) polyunsaturated fatty acids rapidly modify fatty acid composition and insulin effects in rat adipocytes. *J. Nutr.* **128**: 512-519.

49. Herzberg, G. R., and C. Skinner. 1997. Differential accumulation and release of long-chain n-3 fatty acids from liver, muscle, and adipose tissue triacylglycerols. *Can. J. Physiol. Pharmacol.* **75**: 945-951.

50. Luo, J., S. W. Rizkalla, J. Boillot, C. Alamowitch, H. Chaib, F. Bruzzo, N. Desplanque, A. M. Dalix, G. Durand, and G. Slama. 1996. Dietary (n-3) polyunsaturated fatty acids improve adipocyte insulin action and glucose metabolism in insulin-resistant rats: relation to membrane fatty acids. *J. Nutr.* **126**: 1951-1958.

51. D'Andrea, S., H. Guillou, S. Jan, D. Catheline, J. N. Thibault, M. Bouriel, V. Rioux, and P. Legrand. 2002. The same rat Delta6-desaturase not only acts on 18- but also on 24-carbon fatty acids in very-long-chain polyunsaturated fatty acid biosynthesis. *Biochem. J.* **364**: 49-55.

52. Cunnane, S. C. 2003. Problems with essential fatty acids: time for a new paradigm? *Prog. Lipid Res.* **42**: 544-568.

53. Laiglesia, L. M., S. Lorente-Cebrian, P. L. Prieto-Hontoria, M. Fernandez-Galilea, S. M. Ribeiro, N. Sainz, J. A. Martinez, and M. J. Moreno-Aliaga. 2016. Eicosapentaenoic acid promotes mitochondrial biogenesis and beige-like features in subcutaneous adipocytes from overweight subjects. *J Nutr Biochem* **37**: 76-82.

54. Zhao, M., and X. Chen. 2014. Eicosapentaenoic acid promotes thermogenic and fatty acid storage capacity in mouse subcutaneous adipocytes. *Biochem. Biophys. Res. Commun.* **450**: 1446-1451.

55. Muhlhausler, B. S., R. Cook-Johnson, M. James, D. Miljkovic, E. Duthoit, and R. Gibson. 2010. Opposing effects of omega-3 and omega-6 long chain polyunsaturated Fatty acids on the expression of lipogenic genes in omental and retroperitoneal adipose depots in the rat. *J Nutr Metab* **2010**.

56. Martinez-Fernandez, L., L. M. Laiglesia, A. E. Huerta, J. A. Martinez, and M. J. Moreno-Aliaga. 2015. Omega-3 fatty acids and adipose tissue function in obesity and metabolic syndrome. *Prostaglandins Other Lipid Mediat.* **121**: 24-41.

57. Massaro, M., A. Habib, L. Lubrano, S. Del Turco, G. Lazzerini, T. Bourcier, B. B. Weksler, and R. De Caterina. 2006. The omega-3 fatty acid docosahexaenoate attenuates endothelial cyclooxygenase-2 induction through both NADP(H) oxidase and PKC epsilon inhibition. *Proc. Natl. Acad. Sci. U. S. A.* **103**: 15184-15189.

58. Kim, M., T. Goto, R. Yu, K. Uchida, M. Tominaga, Y. Kano, N. Takahashi, and T. Kawada. 2015. Fish oil intake induces UCP1 upregulation in brown and white adipose tissue via the sympathetic nervous system. *Sci. Rep.* **5**: 18013.

59. Pahlavani, M., F. Razafimanjato, L. Ramalingam, N. S. Kalupahana, H. Moussa, S. Scoggin, and N. Moustaid-Moussa. 2017. Eicosapentaenoic acid regulates brown adipose

tissue metabolism in high-fat-fed mice and in clonal brown adipocytes. *J Nutr Biochem* **39**: 101-109.

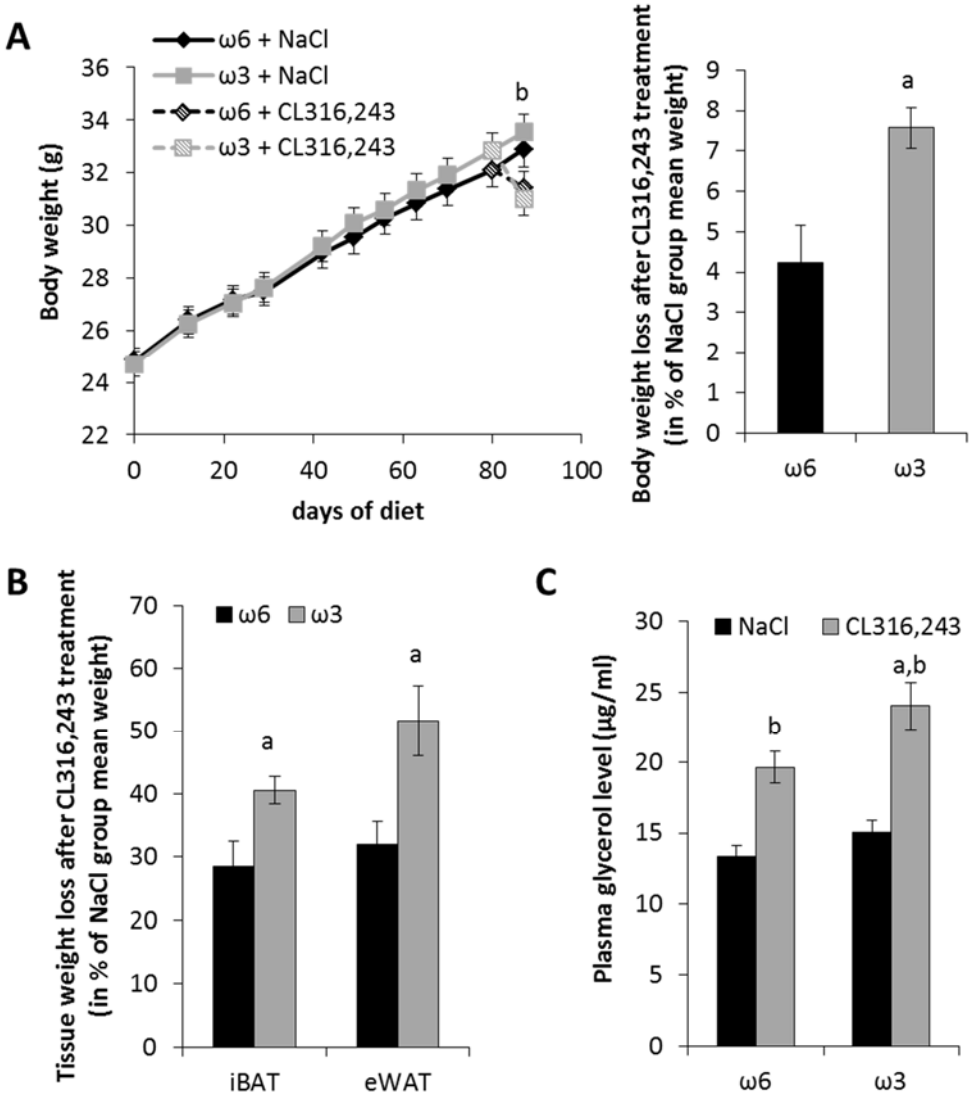

Figure 1. A low dietary ω6/ω3 ratio enhances body weight loss in response to a β3-adrenergic receptor agonist. Mice were fed with diets supplemented with ω6 PUFAs or ω3 PUFAs, respectively, at 28°C during 12 weeks. CL316,243 or vehicle (NaCl) treatment was performed daily during the last week of feeding. A) Left: Body weight development of mice; Right: body weight loss of mice after CL316,243 treatment relative to vehicle treatment. B) Interscapular brown adipose tissue (iBAT) and epididymal white adipose tissue (eWAT) weight loss after CL316,243 treatment. C) Plasma glycerol levels after NaCl or CL316,243 treatment. Data are displayed as the mean ± SEM, n = 12 mice per group. a = $p<0.01$ ω6 *vs* ω3 and b = $p<0.01$ NaCl *vs* CL316,243.

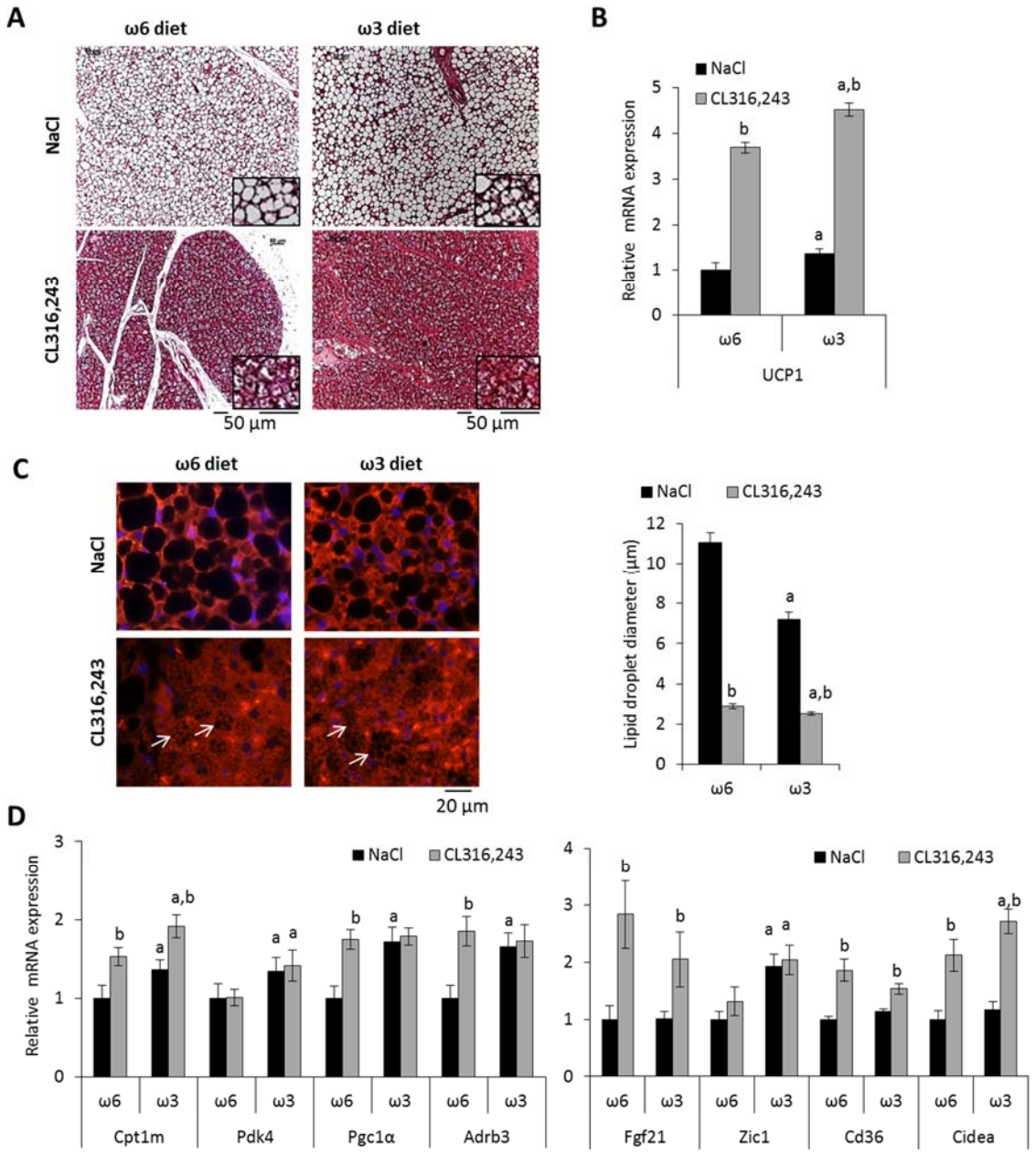

Figure 2. Morphological and molecular analysis of brown adipose tissue. A) 2 and (B) expression of Ucp1 mRNA. C) PLN1 immunostaining of iBAT sections from mice fed ω6 or ω3-diet. Lipid droplet (white arrows) diameters were evaluated using PLN1 staining, data are displayed as mean ± sem, n = 200 lipid droplets/mice, 4 mice per group. D) Expression of brown adipocyte marker mRNAs was determined by RT-qPCR. mRNA expressions are expressed as fold increase relative to "NaCl-ω6" values and are represented as a mean ± SEM, n = 12 mice per group. a = $p<0.01$ ω6 *vs* ω3 and b = $p<0.01$ NaCl *vs* CL316,243.

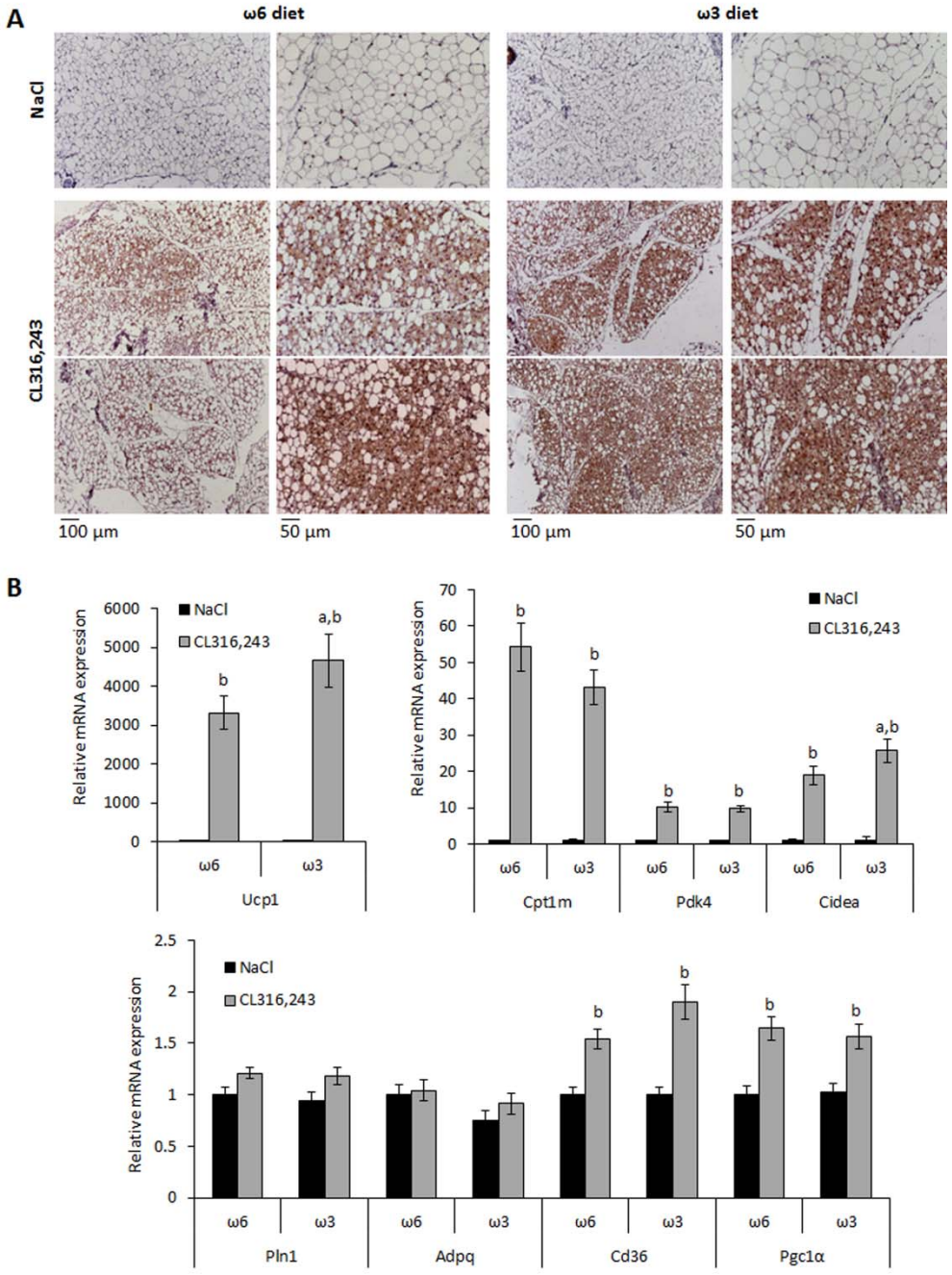

Figure 3. Morphological and molecular analysis of sub-cutaneous white adipose tissue. A) UCP1 immunohistological analysis of sub-cutaneous WAT (scWAT) sections from mice fed ω6 or ω3-diet. Slides were counter-stained with hematoxylin and eosin. B) Expression of Ucp1 and brite/white adipocyte marker mRNAs was determined by RT-qPCR. mRNA expressions are expressed as fold increase relative to "NaCl-ω6" values and are presented as mean ± SEM, n = 12 mice per group. a = $p<0.01$ ω6 *vs.* ω3 and b = $p<0.01$ NaCl *vs* CL316,243.

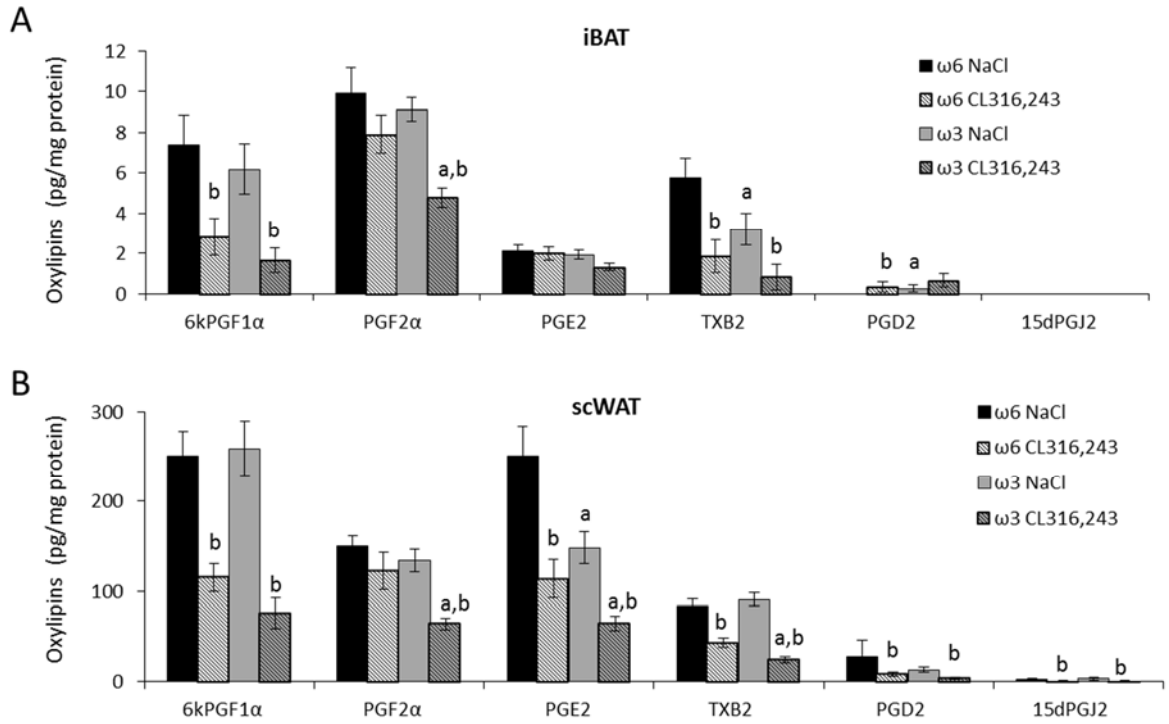

Figure 4. Abundance of ω6 PUFA-derived eicosanoids in BAT and WAT. Eicosanoid levels were measured by LC-MS/MS in (A) iBAT and (B) scWAT of vehicle and CL316,243-treated mice fed with ω6 and ω3 diet. Data are presented as mean ± SEM of 8 mice per group. a = $p<0.01$ ω6 *vs* ω3 and b = $p<0.01$ NaCl vs CL316,243.

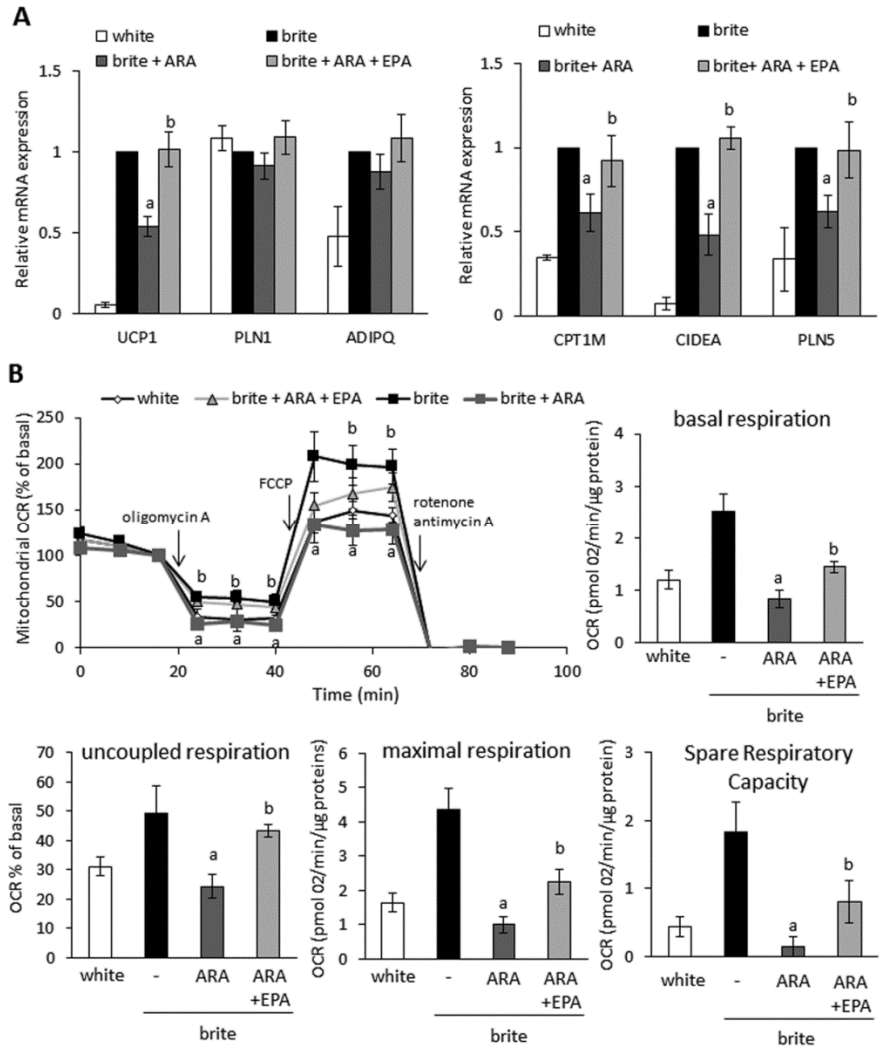

Figure 5. EPA reversed the effect of ARA on adipocyte browning *in vitro*. hMADS cells were differentiated into white or brite adipocytes. Brite hMADS adipocytes were treated during the last 3 days of differentiation with 10 µM ARA in the presence or absence of 3.3 µM EPA. A) Expression of adipocyte markers was determined by RT-qPCR and is expressed as fold increase relative to "brite" group values. B) Basal, ATP synthase uncoupled respiration (= % of residual respiration after addition of ATP synthase inhibitor oligomycin A) and maximal respiration (obtained after addition of the chemical uncoupling agent FCCP) were assessed at the end of treatment to determine the oxygen consumption rate (OCR) of mitochondria. The spare respiratory capacity represents a measure for the full respiratory potential of mitochondria and is calculated as the difference between maximal and basal respiration. Data are presented as mean ± SEM of 3 (A) or 6 (B) independent experiments. a = $p<0.01$ *vs* brite and b = $p<0.01$ *vs* brite + ARA.

JOURNAL OF LIPID RESEARCH

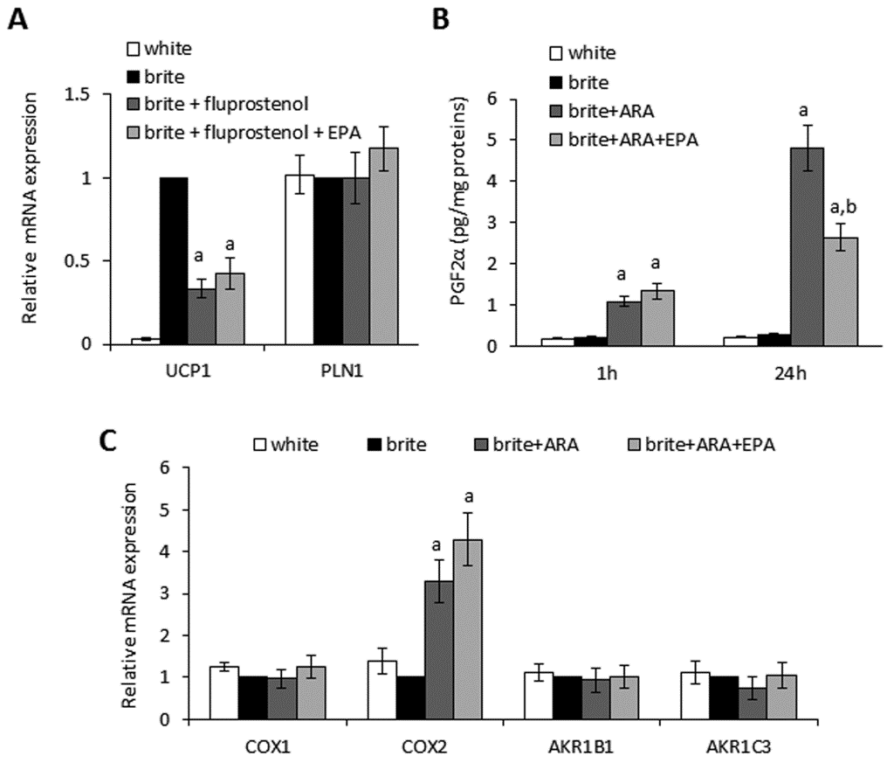

Figure 6. EPA competes with ARA at the cyclooxygenase level. hMADS cells were differentiated into white or brite adipocytes. A) Brite hMADS adipocytes were treated with 10 nM fluprostenol (agonist of PGF2α receptor) in the presence or absence of 3.3 µM EPA during the last 3 days of adipogenic differentiation. UCP1 and PLN1 were evaluated by RT-qPCR. B) Brite hMADS were exposed to 10 µM ARA in the presence or absence of 3.3 µM EPA for 1 or 24 h. PGF2α was quantified in culture media by EIA. C) Brite hMADS adipocytes were treated with 10 µM ARA in the presence or absence of 3.3 µM EPA during the last 3 days of differentiation. Expression of enzymes involved in the metabolization of ARA to PGF2α was evaluated by RT-qPCR. mRNA expressions are expressed as fold increase relative to "brite" values and are presented as mean ± SEM of 3 independent experiments. a = $p<0.01$ *vs* brite and b = $p<0.01$ *vs* brite + ARA.